2013 IEEE 10th International Symposium on Biomedical Imaging:
From Nano to Macro
San Francisco, CA, USA, April 7-11, 2013

NEUROELECTROMAGNETIC IMAGING OF CORRELATED SOURCES USING A NOVEL SUBSPACE PENALIZED SPARSE LEARNING

Jae Jun Yoo[a], Jongmin Kim[a], Chang-Hwan Im[b], and Jong Chul Ye[a]

[a]Bio Imaging & Signal Processing Lab., Dept. of Bio& Brain Engineering, KAIST
291 Daehak-ro, Yuseong-gu, Daejon 305-701, Republic of Korea
[b]Dept. of Biomedical Engineering, Hanyang University, Seoul 133-791, Republic of Korea

ABSTRACT

Localization of brain signal sources from EEG/MEG has been an active area of research [1]. Currently, there exists a variety of approaches such as MUSIC [2], M-SBL [3], and etc. These algorithms have been applied for various clinical examples and demonstrated excellent performances. However, when the unknown sources are highly correlated, the conventional algorithms often exhibit spurious reconstructions. To address the problem, this paper proposes a new algorithm that generalizes M-SBL by exploiting the fundamental subspace geometry in the multiple measurement problem (MMV). Experimental results using simulation and real phantom data show that the proposed algorithm outperforms the existing methods even under a highly correlated source condition.

Index Terms— EEG/MEG source imaging, joint sparse recovery, MUSIC, M-SBL

1. INTRODUCTION

Electroencephalography and magenetoencephalography (EEG /MEG) are noninvasive techniques using external electromagnetic signal measurements [1]. They provide a good temporal resolution over the functional MRI (fMRI) and positron emission tomography (PET) with a potential to detect the millisecond timescale of neural population activities. However, estimating the location and distribution of the current sources from electromagnetic recordings requires the solution of ill-posed inverse problem. In EEG/MEG, a forward modeling which defines the relationship between head currents and the electromagnetic fields is described by Biot-Savart law [1]. Mathematically, it can be stated as

$$\begin{bmatrix} \mathbf{y}_1 \\ \vdots \\ \mathbf{y}_m \end{bmatrix} = [A_{1,x}, A_{1,y}, A_{1,z}, A_{2,x}, \cdots, A_{n,z}] \begin{bmatrix} \mathbf{x}_1 \\ \vdots \\ \mathbf{x}_{3n} \end{bmatrix} + \boldsymbol{\epsilon} \quad (1)$$

This work was supported by the National Research Foundation of Korea(NRF) grant No. 20120000173 funded by the Korea government(MEST). JCY would like to thank Prof. Yoram Bresler at Univ. of Ilinois for helpful discussions.

where $\mathbf{y} \in \mathbb{R}^m$ is a vector containing electromagnetic field measurements at the m sensors, $A \in \mathbb{R}^{m\times 3n}$ is an leadfield matrix whose elements are explicitly specified in the model. The columns of A are three times the number of voxels, i.e. $3n$, representing the point dipoles in Cartesian coordinates (x, y, z). Thus, each column $A_{i,j}$ corresponds to *j*th component of a dipole located in the *i*th voxel and each row corresponds to one sensor. Then, the goal in EEG/MEG source imaging problems is to estimate $\mathbf{x}$, given $\mathbf{y}$ and A.

Now suppose that multiple response vectors have been collected over N snapshots with an equivalent leadfield matrix A. Such a situation is common in EEG/MEG recordings and various applications [2] [3]. Then, the multiple response model becomes

$$Y = AX + E \quad (2)$$

where $Y \in \mathbb{R}^{m\times N}$, $X \in \mathbb{R}^{3n\times N}$, and $E \in \mathbb{R}^{m\times N}$. Up to a certain number of snapshots, we can assume that the source locations are relatively stationary. Moreover, for example, epileptic sources are usually sparsely distributed, so the problem can be formulated as the following multiple measurement vector problem or joint sparse recovery problem:

$$\min_X \|X\|_0 \quad \text{subject to } \|Y - AX\|_F < \delta \quad (3)$$

where $\|X\|_0$ denotes the number of non-zero rows.

Many advanced reconstruction methods are currently available, which includes multiple signal classification (MUSIC) [2], multiple sparse Bayesian learning (M-SBL) [3], and etc. However, when the unknown sources are highly correlated, these algorithms often exhibits either blurry or spurious reconstructions. To address the problem, this paper proposes a new algorithm that generalizes M-SBL by exploiting the subspace geometry in MMV. More specifically, this algorithm replaces the $\log|\cdot|$ term in M-SBL with a new rank penalty that is more suitable for minimizing in the context of MMV. Theoretical analysis demonstrates that even though M-SBL is often impossible to remove all local minimizers, the proposed method can do that under fairly mild conditions, without affecting the global minimizer. We perform simulation studies and real experiments to validate the proposed algorithm. Our results demonstrate that the proposed algorithm can provide significantly improved reconstruction in various conditions.

2. SUBSPACE PENALIZED SPARSE LEARNING

2.1. M-SBL: A Review

Under appropriate assumptions of noise and signal Gaussian statistics, one can show that M-SBL minimizes the following cost function in a so-called $\boldsymbol{\gamma}$ space [4]:

$$\mathcal{L}^{\gamma}(\boldsymbol{\gamma}) = \mathrm{Tr}\left(\Sigma_y^{-1} Y Y^*\right) + N \log |\Sigma_y| \tag{4}$$

where $\Sigma_y = \lambda I + A\Gamma A^*$ and $\Gamma = \mathrm{diag}(\boldsymbol{\gamma})$, which is equivalent to the following standard sparse recovery framework [4]:

$$\min_X \mathcal{L}^{\mathbf{x}}(X), \quad \mathcal{L}^{\mathbf{x}}(X) = \|Y - AX\|_F^2 + \lambda g_{msbl}(X) \tag{5}$$

where $g_{msbl}(X)$ is a penalty given by

$$g_{msbl}(X) \equiv \min_{\boldsymbol{\gamma} \geq \mathbf{0}} \mathrm{Tr}\left(X^* \Gamma^{-1} X\right) + N \log |\lambda I + A\Gamma A^*| \,. \tag{6}$$

Wipf *et al* [4] proposed an alternating minimization approach with respect to X and $\boldsymbol{\gamma}$ to solve the minimization problem (5). Such derivation of M-SBL is equivalent to the original derivation using Bayesian approaches.

2.2. Subspace Penalized Sparse Learning

In order to develop a new joint sparse recovery algorithm that improves M-SBL, we need to understand the roles of the regularization term in M-SBL. It turns out that $\log |\lambda I + A\Gamma A^*|$ works a good (non-convex) proxy for $\mathrm{rank}(A\Gamma^{\frac{1}{2}})$, and the penalty imposes a sparsity in the selected sub-matrix. However, the following theorem shows that rather than minimizing the $\mathrm{rank}(A\Gamma^{\frac{1}{2}})$, there exists another rank penalty that is more suitable for minimizing in the context of MMV.

Theorem 2.1 *Suppose that we are given a* noiseless *observation matrix $Y \in \mathbb{R}^{m \times N}$, and let $R(Q) = R^{\perp}(Y)$. Assume that $A \in \mathbb{R}^{m \times n}$, $X_* \in \mathbb{R}^{n \times r}$, $Y \in \mathbb{R}^{m \times r}$ satisfy $AX_* = Y$ where $\|X_*\|_0 = k$ and the columns of Y are linearly independent and $r = \mathrm{rank}(Y)$. If A satisfies a restricted isometry property (RIP) condition $0 \leq \delta^L_{2k-r+1}(A) < 1$, then for noiseless measurement we have*

$$k - r = \min_{|I| \geq k} \mathrm{rank}\left(Q^* A_I\right),$$

and the corresponding support set I_* is equivalent to $\mathrm{supp} X_*$.

Theorem 2.1 indicates that by minimizing a new rank prior, we can obtain the true sparse support. Hence, we propose the following penalty to replace $g_{msbl}(X)$ in (5):

$$g_{SPL,\epsilon}(X) \equiv \min_{\boldsymbol{\gamma} \geq \mathbf{0}} \mathcal{G}_{SPL,\epsilon}(\boldsymbol{\gamma}, X) \tag{7}$$

where

$$\mathcal{G}_{SPL,\epsilon}(\boldsymbol{\gamma}, X) = \mathrm{Tr}\left(X^* \Gamma^{-1} X\right) + N \log |Q^* A\Gamma A^* Q + \epsilon I| \tag{8}$$

Due to the non-negativity constraint for $\boldsymbol{\gamma}$, a critical solution should satisfy the fist order Karush-Kuhn-Tucker (KKT) necessary conditions. Accordingly, we can derive an alternating minimization method using a fixed point update. More specifically, for a given estimate $\boldsymbol{\gamma}^{(t)}$, we have :

$$X^{(t+1)} = \Gamma^{(t)} A^* (\lambda I + A\Gamma^{(t)} A^*)^{-1} Y, \quad \Gamma^{(t)} = \mathrm{diag}(\boldsymbol{\gamma}^{(t)}).$$

For a given $X^{(t)}$, we have the following update equation:

$$\gamma_i^{(t)} = \left(\frac{\frac{1}{N} \sum_j |x_{ij}^{(t)}|^2}{\mathbf{a}_i^* Q (Q^* A \Gamma^{(t)} A^* Q + \epsilon I)^{-1} Q^* \mathbf{a}_i} \right)^{\frac{1}{2}} . \tag{9}$$

2.3. Theoretical Result on Local Minimizers

In [4], Wipf provided a condition to remove all local minimizer for the case of SBL. We can extend the results and show that the conditions for removing local minimizers are more favorable for the proposed method than for M-SBL.

Theorem 2.2 *Let X_* denote a maximally sparse solution to be $Y = AX_*$ with $\|X_*\|_0 = k$. Let A satisfy the RIP condition with $0 \leq \delta^L_{2k-r+1}(A) < 1$, where $r = \mathrm{rank}(Y)$. Suppose X represent a coefficient such that $S = \mathrm{supp} X$ and $k < |S| = p \leq m$, and $X^S = A_S^{\dagger} Y$. Let $\Psi = (Q^* A\Gamma A^* Q + \epsilon I)^{-1}$ and the subscript $\backslash i$ denotes the corresponding matrix by removing the i-th columns of the matrix A. Then, the following statements are true:*

1. *For some $j \notin S$, if we have*

$$\mathbf{v}_{S,j}^* \left(\bar{W}_{S,j} \bar{R}_S \bar{W}_{S,j}\right) \mathbf{v}_{S,j} > 1, \tag{10}$$

where $\mathbf{v}_{S,j} = A_S^{\dagger} \mathbf{a}_j$, $\bar{R}_S = [\bar{r}_{ii'}]_{i,i' \in S}$ and $\bar{W}_{S,j} = \mathrm{diag}([\bar{w}_i]_{i \in S})$ such that

$$\bar{r}_{ii'} = \frac{\mathbf{x}^i (\mathbf{x}^{i'})^*}{\|\mathbf{x}^i\| \|\mathbf{x}^{i'}\|}, \quad \bar{w}_i = \sqrt{\frac{\mathbf{a}_i^* Q \Psi_{\backslash i} Q^* \mathbf{a}_i}{\mathbf{a}_j^* Q \Psi Q^* \mathbf{a}_j}}, \tag{11}$$

for $i, i' \in S$ and $j \notin S$, then X is not *a local minimizer.*

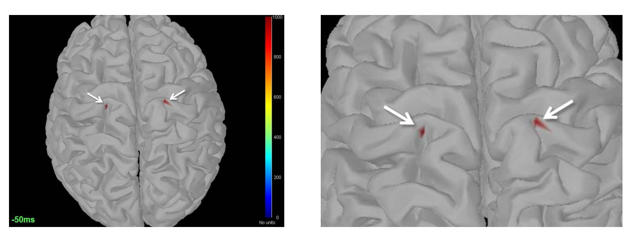

(a) (b)

Fig. 1. (a) Ground-truth of the source image and (b) its magnified view.

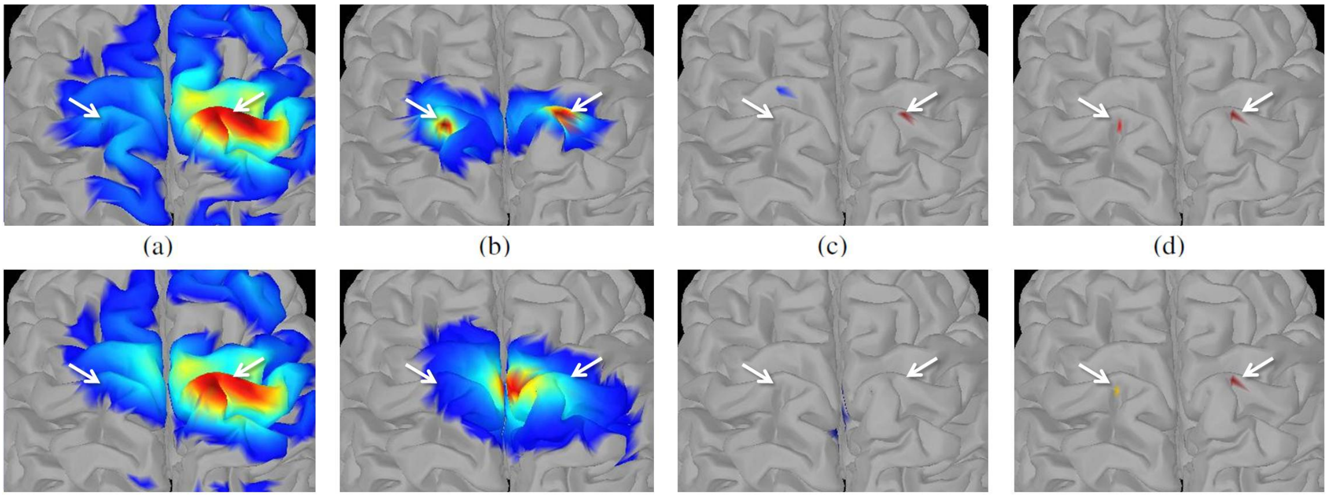

(a) (b) (c) (d)

(e) (f) (g) (h)

Fig. 2. Simulation results from uncorrelated and correlated input signals with noise (SNR = 35dB) using (a,e) minimum norm, (b,f) MUSIC, (c,g) M-SBL, and (d,h) proposed algorithm. Top row indicates the results from uncorrelated sources, whereas the bottom row corresponds to the correlated sources.

2. *In particular, if* $\mathrm{rank}(Q^* A_S) \leq m - r$ *and* $|S \cap \mathrm{supp} X_*| \geq k - r$*, then there always exists* $\epsilon_1 > 0$ *such that for any* $0 < \epsilon < \epsilon_1$*,* X *is* not *a local minimizer.*

Our local minimizer analysis clearly show why the proposed method is better than M-SBL. More specifically, as long as $k - r$ correct supports are included in a local minimizer, the proposed method can escape from the local minimizer. In addition, the proposed method is more robust to the condition number of the unknown signal X compared to M-SBL. More specifically, in (10), $\mathrm{rank}(\bar{R}_S) \leq k$, so there always exist null spaces when the rank of $\bar{R}_S$ is not full. In particular, in noisy cases, the corresponding numerical rank can be reduced when the condition number of $\bar{R}_S$ is bad, which can happen when the rows of X^S are highly correlated. In this case, there are more chances that $\bar{W}_{S,j}\mathbf{v}_{S,j}$ can fall into the null space so that the condition (10) cannot be met. However, in the proposed method, we can still prevent such situation as long as $k - r$ correct support are included in X^S.

2.4. Extension to Dipole Moment

For easier understanding so far we have explained the proposed algorithm under a simplified assumption that the lead field matrix is $m \times n$ assuming that the source is a scalar rather than a three-dimensional vector. However, equivalent derivation can be easily obtained for $m \times 3n$ cases with considering block structure for dipole moments. Indeed, our experimental results are generated using an algorithm derived by exploiting $m \times 3n$ block sparse structure.

3. EXPERIMENTAL RESULTS

3.1. Simulation Results

In our simulation, a leadfield matrix was generated by Brainstorm [5]. Then, an unknown signal X with $\mathrm{rank}(X) = r \leq k$ was randomly generated. After generating noiseless data, we added zero mean white Gaussian noise to have $SNR = 35dB$ measurements. The simulation parameters were as follows: $m = 151, n = 24220$, and $N = 375$, respectively.

Fig.1 is the ground truth image of the source location. To compare the proposed algorithm with various recovery methods, the recovery results of minimum norm, MUSIC, and M-SBL are shown in Fig.2. As can be seen in Fig.2 top row, all algorithms recovered the correct source locations when the signals were uncorrelated; however, noticeable improvement in spatial resolution can be still observed using the proposed algorithm. Moreover, for the case of correlated signals, the proposed method provides correct locations whereas the other algorithms fail.

3.2. Real Experiments

Head phantom was made in Hanyang University for algorithm validation. A conductive skull was not available so 17 electrodes are attached inside the skull under international 10-20 system (except A1 and A2) and then using coaxial cable, three signal sources (S1,S2, and S3) are positioned at different locations and directions (Fig.3). Sensor location, source location, and head surface point data for BEM (boundary element model) were obtained using a 3D digitizer. Skull phantom was filled with physiological saline solution which has a similar conductance with the CSF to measure the data. Correlated sinusoidal waves are generated as input signals by a function generator and the head phantom data was gathered by an amplifier as shown in Fig.3(b). Leadfield matrix, $A \in \mathbb{R}^{m \times 3n}$, was obtained by CURRY 7.0 (CURRY, Compumedics/Neuroscan El Paso, TX, USA) where the experimental parameters were $m = 17, n = 26290$, and $N = 375$.

For the single source case, all the methods provided correct source images (results not shown). However, as shown in Fig.4, for the case of two correlated sources at S2 and S3, the proposed method provides accurate locations whereas all other methods fail. For example, M-SBL identified only one source locations, and the minimum norm and MUSIC provided very blurry reconstruction. However, the proposed method accurately identified the correlated two source locations. Note that the true source locations are indicated with red circles (Fig. 4).

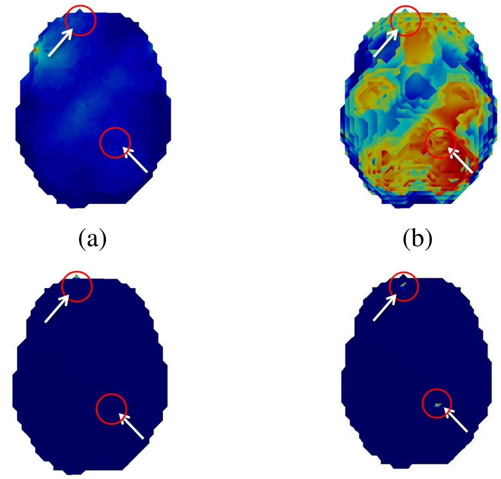

(a) (b) (c) (d)

Fig. 4. Real experimental results from two correlated sources at S2 and S3 using (a) minimum norm, (b) MUSIC, (c) M-SBL (d) proposed algorithm.

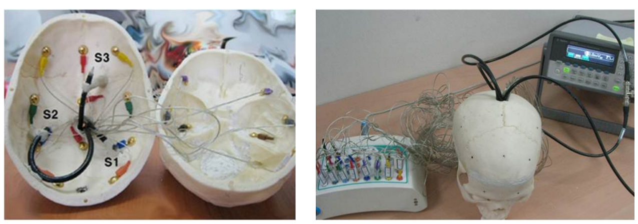

(a) (b)

Fig. 3. Skull phantom : (a) inside view, and (b) outside view.

4. CONCLUSIONS

In this paper, we proposed a novel subspace penalized sparse learning algorithm by exploiting the rank reduction property discovered in subspace based joint sparse recovery algorithms. Compared to M-SBL, theoretical analysis showed that the proposed method avoids more local minimizers and less prone to correlated signal sources. Furthermore, the algorithm can be easily implemented using an alternating minimization methods that has very similar structures as M-SBL. Experimental results demonstrated that our proposed algorithm improved the source recovery over the conventional methods such as MUSIC, minimum norm, and M-SBL algorithms under both a highly correlated and uncorrelated source conditions.

5. REFERENCES

[1] S. Baillet, J.C. Mosher, and R.M. Leahy, "Electromagnetic brain mapping," *IEEE Signal Processing Magazine*, vol. 18, no. 6, pp. 14–30, 2001.

[2] J.C. Mosher, P.S. Lewis, and R.M. Leahy, "Multiple dipole modeling and localization from spatio-temporal meg data," *IEEE Trans. on Biomedical Engineering*, vol. 39, no. 6, pp. 541–557, 1992.

[3] D.P. Wipf and B.D. Rao, "An empirical bayesian strategy for solving the simultaneous sparse approximation problem," *IEEE Trans. on Signal Processing*, vol. 55, no. 7, pp. 3704–3716, 2007.

[4] D. Wipf, B. Rao, and S. Nagarajan, "Latent variable bayesian models for promoting sparsity," *IEEE Trans. on Information Theory*, vol. 57, no. 9, pp. 6236, 2011.

[5] F. Tadel, S. Baillet, J.C. Mosher, D. Pantazis, and R.M. Leahy, "Brainstorm: a user-friendly application for MEG/EEG analysis," *Computational Intelligence and Neuroscience*, vol. 2011, pp. 8, 2011.